

## Extremely Low Ionospheric Peak Altitudes in the Polar-Hole Region

Robert F. Benson and Joseph M. Grebowsky  
Laboratory for Extraterrestrial Physics  
NASA/Goddard Space Flight Center  
Greenbelt, MD 20771

### ABSTRACT

Vertical electron-density ( $N_e$ ) profiles, deduced from newly-available ISIS-II digital ionospheric topside-sounder data, are used to investigate the "polar-hole" region within the winter, nighttime polar cap ionosphere during solar minimum. The hole region is located around 0200 MLT near the poleward side of the auroral oval. Earlier investigations had revealed very low  $N_e$  values in this region (down to  $200 \text{ cm}^{-3}$  near 300 km). In the present study, such low  $N_e$  values ( $\approx 100 \text{ cm}^{-3}$ ) were only found near the ISIS-II altitude of 1400 km. The peak ionospheric concentration below the spacecraft remained fairly constant ( $\sim 10^5 \text{ cm}^{-3}$ ) across the hole region but the altitude of the peak dropped dramatically. This peak dropped, surprisingly, to the vicinity of 100 km. These observations suggest that the earlier satellite *in situ* measurements, interpreted as deep holes in the ionospheric F-region concentration, could have been made during conditions of an extreme decrease in the altitude of the ionospheric  $N_e$  peak. The observations, in combination with other data, indicate that the absence of an F-layer peak may be a frequent occurrence at high latitudes.

## INTRODUCTION

The magnetic polar cap is the region poleward of the auroral oval in each hemisphere. In the winter it is subject to prolonged periods of darkness and has lower electron densities ( $N_e$ ) than in the oval ionosphere. It is characterized by  $N_e$  enhancements (tongues, patches and blobs) and depletions (troughs, cavities and holes). Ignoring the complex time-dependent structures, the average  $N_e$  in the polar cap decreases during the winter night from noon to midnight as the plasma convects antisunward chemically decaying in the absence of photoionization. If convection is slow, deep ionization holes develop.

We here focus on the polar-cap region where deep holes had been detected previously near 300 km. The initial work on these ionization holes, by *Brinton et al.* [1978], was based on Atmospheric Explorer C (AE-C) winter nighttime ion-composition data. They found extremely low  $O^+$  ion densities that were several orders of magnitude less than typical polar-cap ion densities (reaching as low as  $200 \text{ cm}^{-3}$  at 310 km). The deepest ones were observed in the southern-hemisphere (often over horizontal distances exceeding 100 km) during solar minimum conditions. Such low ion densities have not been reported in other satellite investigations.

*Hoegy and Grebowsky* [1991] used AE-C and Dynamics Explorer 2 (DE 2) Langmuir probe data to statistically investigate the dependence of the ionization hole-region  $N_e$  on solar activity, universal time (UT), magnetic activity, season and the hemisphere of observation. Strong dependencies on solar activity (as described by the F10.7 cm solar flux) and UT were found but there was only a weak dependency on magnetic activity (described by the  $Kp$  index). The hole region  $N_e$  increased with increasing F10.7 and was, on average, about a factor of 10 larger in the northern hemisphere than in the southern hemisphere.

*Doe et al.* [1993] using Sondre Stromfjord incoherent scatter radar scans during overpasses of the HILAT and Polar Bear satellites (which occasionally provided coincident UV images, total electron content and magnetometer measurements) identified narrow depletions (horizontal dimensions less than 100 km) which they called auroral ionospheric cavities. They were associated with downward directed electric currents. These northern-hemisphere features, observed during periods of moderate magnetic activity, had  $N_e$  depletions of 20 to 70% below surrounding values which, on average, were  $7.8 \times 10^4 \text{ cm}^{-3}$ . They were observed just poleward of the statistical auroral oval and were co-located in the hole region delineated by *Brinton et al.* [1978], as illustrated in Figure 1.

*Crowley et al.* [1993] investigated the morphology and evolution of the polar-hole region above Greenland using a digital ionosonde, a 250 MHz scintillation receiver and simultaneous *in situ* measurements by the Defense Meteorological Satellite Program F8 and F9 satellites. This investigation was conducted during quiet magnetic conditions ( $Kp = 1^+$ ) during solar maximum. The *in situ* satellite measurements detected ion densities as low as  $10^3 \text{ cm}^{-3}$  at 840 km inside an  $N_e$  hole. The ground-based ionosonde enabled them to determine the electron-density altitude profile  $N_e(h)$  up to the altitude of the F-layer peak and to determine the altitude and maximum  $N_e$  at the peak (often referred to as  $h_{\text{max}}$  and  $N_e(\text{max})$ , respectively). In one of the two polar holes encountered during their 24-hr experimental run, ionosonde observations indicated  $N_e(\text{max})$  decreased by a factor of four within the hole. They also observed an increase in  $h_{\text{max}}$  by about 10% within the holes relative to the surrounding values and noted that  $h_{\text{max}}$  often exceeded 300 km in the holes.

In this paper we present observations that add a new aspect to the physics of the hole region. The observations are based on newly-available ISIS-II digital ionospheric topside-sounder data

(<http://nssdc.gsfc.nasa.gov/space/isis/isis-status.html>) which are used to produce  $N_e(h)$  profiles from the satellite altitude down to  $h_{\max}$  in the hole region. These profiles are used to estimate  $h_{\max}$  and  $N_e(\max)$  which are important parameters for understanding the formation of holes and their structure. They are usually presumed to correspond to an F-layer peak. At high latitudes, however, there are times when there is no evidence of an F-layer peak and  $h_{\max}$  and  $N_e(\max)$  correspond to an ionization peak at altitudes usually associated with the E region [Bates and Hunsucker, 1974; Prikryl et al., 1999]. We will show ISIS-II topside-sounder data that indicates that such  $N_e(h)$  profiles are present in the polar-hole region described above and in other high-latitude regions.

## OBSERVATIONS

A survey was made of available ISIS-II digital topside-sounder ionograms in the 70 to 90° invariant-latitude region for magnetic local times between 2300 and 0400 to locate data within the hole region delineated in the earlier studies (Figure 1). Three ISIS-II northern-hemisphere passes through this region in 1976, during sunspot-minimum winter conditions, were selected. The time periods for these data, and for the data of the earlier investigations discussed in the previous section, are indicated on a plot of solar activity in Figure 2.

Three ISIS-II ionograms from one of the passes through the polar hole region are reproduced in Figure 3. Each shows local plasma resonances (at the top) and remote ionospheric reflection traces embedded in scatter returns commonly referred to as spread F. The resonance just beyond 0.1 MHz on each ionogram occurs at the electron plasma frequency, indicating that  $N_e$  exceeds  $124 \text{ cm}^{-3}$  at the satellite altitude of 1400 km. The  $N_e(h)$  profiles deduced from these ionograms, using the inversion algorithm developed by Jackson [1969], are shown in Figure 4. By combining sequential  $N_e(h)$  profiles obtained along the pass, an  $N_e$  contour plot was created and is

presented in the top panel of the left column of Figure 5. The middle and bottom panels in the left column of Figure 5 present the corresponding  $N_e(\text{max})$  and  $h_{\text{max}}$  values, respectively. Note that the former remains practically unchanged whereas the latter decreases dramatically in the hole region around 1902 UT.

The results from the other two ISIS-II passes processed to produce  $N_e(h)$  profiles are shown in the center and right columns of Figure 5. Both show similar behavior in the hole regions but the  $h_{\text{max}}$  values are not as depressed as in the pass discussed above. The pass shown in the center column reveals the lowest overall  $N_e$  values of the three passes (at all altitudes) as the satellite crosses the polar cap and enters the hole region (near the low  $h_{\text{max}}$  values just prior to 1018 UT) from the high-latitude side. The erratic behavior of  $h_{\text{max}}$  between approximately 1018 and 1021:30 UT is due to interference on the ionograms which prevented reliable scaling of the high-frequency portions of the ionogram traces. The low  $h_{\text{max}}$  values after about 1022 UT correspond to the equatorward-moving satellite entry into the auroral-oval/main-trough [Muldrew, 1965] region. The interpretation of the ionograms in this region was also compromised by interference in addition to weak multiple traces with spread F. The ionospheric-reflection traces on the last ionogram of this sequence, where the calculated  $h_{\text{max}}$  value was below 100 km, were particularly weak. The results for the third pass investigated, presented in the right column of Figure 5, reveals two regions of reduced  $h_{\text{max}}$  values: one on the dayside near the cusp region (0737 UT) and one within the average polar hole location (as identified in Figure 1) at 0747 UT. In each case, negligible changes in  $N_e(\text{max})$  accompanied the reduced  $h_{\text{max}}$  values.

The  $N_e$  latitudinal resolution is different in the three passes presented in Figure 5. The data in the left column were collected when the sounder was in a mode of operation that produced two

active sounding ionograms followed by two passive ionograms where only the sounder-receiver was in operation. In the top-left panel of Figure 5, the satellite positions are indicated only for the active soundings which produced the data leading to the  $N_e$  profiles (see the open circles at the top of the figure). Since the ionograms were spaced 14 s apart, corresponding to a frequency-sweep range from 0.1 to 10 MHz (see Figure 3), the latitudinal separation of adjacent  $N_e$  profiles obtained from the polar-orbiting ISIS-II sounder was either approximately 100 km or 300 km. During the other two passes represented in Figure 5 (center and right columns), the sounder was operational on every ionogram. These ionograms were also separated by 14 s, so the latitudinal separation between all profiles was approximately 100 km.

The deduced  $h_{\max}$  in the lower three panels of Figure 5 can differ from the true altitude of the ionosphere peak for two reasons. First, the reflection traces on the ionograms may not be of sufficient clarity (due to an inappropriate antenna orientation, interference or spread F) to yield accurate  $N_e$  information all the way down to the true peak. Under these conditions, the deduced  $h_{\max}$  value can be higher than the altitude of the ionization peak. As discussed above, this factor was the likely cause of the erratic behavior of  $h_{\max}$  in the center column of Figure 5. Second, the analysis program assumes vertical propagation in a horizontally-stratified ionosphere. At high latitudes, radio propagation guided along the magnetic-field direction often dominates over vertical propagation. When reflection traces due to such propagation are evaluated using the vertical-propagation assumption, the longer slant ranges lead to calculated reflection-layer altitudes that are too low. In the three polar-hole regions presented in Figure 5, the dip angles (not shown) are large ( $87^\circ$ ,  $85^\circ$  and  $83^\circ$  for the left, center and right columns, respectively) and the error introduced by such possible field-aligned propagation is small (2, 5 and 9 km, respectively). The error could be more significant, however, for the lowest-altitude point in the

lower panel of the center column of Figure 5 where the dip angle is  $76^\circ$ . If field-aligned propagation was involved in the traces used to deduce  $h_{\max}$  in this case, the calculated value shown could be too low by nearly 40 km.

## DISCUSSION

Several different interpretations have been given to explain observations of polar ionospheric depletions. *Brinton et al.* [1978] attributed their AE-C polar-holes to long plasma drift times across a dark polar cap while ionization chemical decay progressed. High plasma drift speeds, which can significantly increase the  $O^+$  chemical loss rate through dissociative recombination, can also produce deep troughs. *Brinton et al.* [1978] ruled this mechanism out on the basis of ion composition and the low plasma temperatures measured in the holes. Similar conclusions about hole formation were reached by *Sojka et al.* [1981a] who theoretically modeled the high-latitude ionosphere under conditions of low magnetic activity at solar minimum. These conditions were selected to compare their results with the data of *Brinton et al.* [1978]. *Sojka et al.* [1981a] were able to show that the polar hole was a natural consequence of competing high-latitude chemical and dynamical processes. Their calculated hole, however, was smaller and in a slightly different location than the average hole location found by *Brinton et al.* [1978]. These differences may have been due to differences between the modeled and observed conditions since *Sojka et al.* [1981a] modeled the northern hemisphere whereas the observations of *Brinton et al.* [1978] corresponded to the southern hemisphere. The model of *Sojka et al.* [1981a] (for low magnetic activity during solar minimum) produced an  $h_{\max}$  value within the hole that was well below 300 km. This value was considerably less than that observed by *Crowley et al.* [1993] (corresponding to low magnetic activity during solar maximum. The latter study found  $h_{\max}$  to increase by 10%

within holes to altitudes above 300 km. Again, the differences may have been caused by differences in the modeled and observed conditions; the former being during solar minimum and the latter during solar maximum. In a later work [Sojka *et al.*, 1981b], the full model calculation was expanded to explore the polar-cap ion composition dependence on variations in magnetic latitude, local time, altitude and UT. They obtained  $O^+$  densities as low as  $200 \text{ cm}^{-3}$  in the hole region at 300 km in agreement with the observations of Brinton *et al.* [1978]. Their predicted  $N_e(h)$  within the polar hole had no F2-region peak; rather,  $N_e(\text{max})$  (of approximately  $2 \times 10^3 \text{ cm}^{-3}$ ) was located at the lower boundary of their model near 150 km. An upgraded version of this global time-dependent ionospheric model was used later in a climatological sense by Sojka *et al.* [1991] to show that it was in agreement with the global AE-C and DE-2 observations of Hoegy and Grebowsky [1991] obtained over one solar cycle. The agreement included the conclusion that the average hole  $N_e$  was about a factor of 10 larger in the northern hemisphere than in the southern hemisphere. Sojka *et al.* [1991] also supported the conclusion of Brinton *et al.* [1978] that the polar hole is formed in regions of weak convection. Doe *et al.* [1993], on the other hand, offered evidence that field-aligned current evacuation was the most attractive explanation for the smaller-scale cavities they observed near the poleward edge of the auroral oval (i.e., smaller-scale relative to the Brinton *et al.* [1978] polar holes). They stressed that these features should not be confused with the polar hole.

The main result of the present investigation is the detection of an extreme decrease in the altitude of the main ionospheric  $N_e$  peak, with a negligible change in the  $N_e$  value at the peak, in the region of polar-cap holes. In one case,  $N_e$  increased monotonically from the satellite altitude of about 1400 km to a maximum near 105 km in the hole (see the dotted curve in Figure 4, corresponding to the  $h_{\text{max}}$  value near 1902:11 UT in the lower left panel of Figure 5). In the other



two cases,  $h_{\max}$  values as low as 155 km and 185 km were observed in the polar-hole regions (near 1017:25 UT and 0746:57 UT in the lower center and lower right panels of Figure 5, respectively).

These decreases observed in  $h_{\max}$  within polar holes in the ISIS-II data are consistent with the predictions of *Sojka et al.* [1981b] and they would lead to "depletions" at a constant altitude of 310 km (appropriate to the AE-C altitude in the *Brinton et al.* [1978] study) of as much as 85% (in the case of Figure 4). Allowing for the factor of 10 difference found between the northern (present ISIS-II study) and the southern [*Brinton, et al.*, 1978] hemispheres found by *Hoegy and Grebowsky* [1991], these results are fairly comparable. The observed decreases in  $h_{\max}$  within the polar holes is not consistent with the observations of *Crowley et al.* [1993]. These differences may have resulted from differences in the observing conditions, e.g., the ISIS-II data used in the present study corresponded to solar minimum (which corresponded to the model conditions used by *Sojka et al.* [1981b]) whereas the work of *Crowley et al.* [1993] corresponded to solar maximum (see Figure 2). Another difference between the present observations and those of *Crowley et al.* [1993] is that  $N_e(\max)$  remained nearly constant throughout the hole region in each of the three passes investigated in the present study whereas *Crowley et al.* [1993] observed a decrease in  $N_e(\max)$  by a factor of four in their long (24 hr) observational monitoring of the hole region. The nearly constant  $N_e(\max)$  values observed over large-scale hole regions in the present study also contrast with the 20 to 70% depletions observed in narrow cavities by *Doe et al.* [1993]. This contrast may be due to the differences in spatial resolution in the two studies since the features observed by *Doe et al.* [1993] were typically less than 100 km in width whereas the latitudinal resolution of the  $N_e$  profiles in the present ISIS-II study is, at best, approximately 100 km as discussed in the previous section.

High-latitude  $N_e$  distributions with very low-altitude peaks have been observed previously. *Bates and Hunsucker* [1974, Fig. 10] observed E-layer peaks near 100 km with no evidence of an F-layer during intense auroral precipitation events with the Chatanika incoherent-scatter radar. *Jelly and Petrie* [1969, Fig. 5] presented an Alouette-1 topside  $N_e$  profile over Alaska showing a monotonic increase in  $N_e$  from 1,000 km to a maximum at 175 km. The ISIS-II experimenters prepared four archived data volumes containing the results of coordinated ionospheric and magnetospheric observations [*Klumpar*, 1980; *Murphree*, 1980; *Shepherd*, 1980; *Burrows et al.*, 1981]. A search of these volumes revealed 89  $N_e$  high-latitude orbit-plane contours, similar to those presented in the top panels of Figure 5. Most of them corresponded to the northern hemisphere during 1971 & 1972. Thus they were recorded several years before the solar-minimum conditions corresponding to the data used in the present study and that of *Brinton et al.* [1978] (see Figure 2). Many of the orbit-plane contours presented in the ISIS-II volumes did not intersect the average hole location shown in Figure 1. Nevertheless, an inspection of all of the  $N_e$  contours was made to compare the minimum altitudes of  $N_e(\text{max})$  with the present results. Even though none of them had  $h_{\text{max}}$  values as low as the 105 km layer seen in Figure 4 and the lower left panel of Figure 5, 13 passes (or 15%) of the ensemble of contours had  $h_{\text{max}} \leq 155$  km (one as low as 120 km) and 22 passes (or 25%) recorded  $h_{\text{max}} \leq 185$  km. More recently, *Prikryl et al* [1999] observed an  $h_{\text{max}} = 115$  km during auroral conditions in Alaska with the OEDIPUS-C bistatic rocket radio sounder. The profile was uniquely determined by a combination of *in situ* and remote measurements based on ionospheric soundings, with the receiver and transmitter separated by 1 km, as the payload descended from its apogee of 824 km. It is important to recall, as stated in the previous section, that the  $h_{\text{max}}$  values determined from topside sounders may be higher than the true altitude of the ionization peak of the  $N_e(h)$  profile.

The present results, combined with the results of these independent studies, suggest that high-latitude regions with a single ionospheric  $N_e$  peak altitude down in the E region may be more common than previously expected. Such profiles may be characteristic features of polar holes at solar minimum and, possibly, the cusp and auroral regions. They would definitely affect the interpretation of *in situ* measurements by a satellite well above the peak altitude. Such a situation is illustrated in the lower left panel of Figure 5 where the dashed horizontal line at 310 km, corresponding to the AE-C altitude during the *Brinton et al* [1978] study, has been added. Thus, an extreme decrease in the altitude of the ionospheric  $N_e$  peak may have contributed to, or been the cause of, the observed reduction in the F-layer densities that were interpreted as deep holes in the ionosphere.

The results also indicate the importance of obtaining the  $N_e(h)$  profile through suspected  $N_e$  depletions and the difficulty of obtaining such profiles. Even though there are uncertainties in the determination of  $h_{\max}$  from topside sounders, the sounding technique provides one of the most powerful tools for such studies because of its ability to perform such measurements globally. *Sojka et al.* [1981b] clearly indicated the difficulty in deducing such profiles based strictly on *in situ* measurements from a satellite in an elliptical orbit.

## SUMMARY

High-latitude ionospheric topside  $N_e$  profiles have revealed extreme decreases in the altitude of the main ionization peak under conditions favorable for the formation of polar-cap holes. The corresponding change in the  $N_e$  value at the peak was negligible. The results, which were based on ISIS-II digital ionograms, suggest that earlier AE-C *in situ* measurements, interpreted as deep ionization holes, may have reflected such decreases in the altitude of the ionospheric peak.

## REFERENCES

- Bates, H. F., and R. D. Hunsucker, Quiet and disturbed electron density profiles in the auroral zone ionosphere, *Radio Sci.*, 9, 455-467, 1974.
- Brinton, H. C., J. M. Grebowsky, and L. H. Brace, The high-latitude winter F region at 300 km: Thermal plasma observations from AE-C, *J. Geophys. Res.*, 83, 4767-4776, 1978.
- Burrows, J. R., L. L. Cogger, and H. G. James, *Coordinated ionospheric and magnetospheric observations from the ISIS 2 satellite by the ISIS 2 experimenters: Volume 4: A. large storms, B. airglow and related measurements, C. VLF observations*, Report No. 81-01, National Space Science Data Center, Greenbelt, Maryland, June, 1981.
- Crowley, G., H. C. Carlson, S. Basu, W. F. Denig, J. Buchau, and B. W. Reinisch, The dynamic ionospheric polar hole, *Radio Sci.*, 28, 401-413, 1993.
- Doe, R. A., M. Mendillo, J. F. Vickrey, L. J. Zanetti, and R. W. Eastes, Observations of nightside auroral cavities, *J. Geophys. Res.*, 98, 293-310, 1993.
- Hoegy, W. R., and J. M. Grebowsky, Dependence of polar hole density on magnetic and solar conditions, *J. Geophys. Res.*, 96, 5737-5755, 1991.
- Jackson, J. E., The reduction of topside ionograms to electron-density profiles, *Proc. IEEE*, 57, 960-976, 1969.
- Jelly, D. H., and L. E. Petrie, The high-latitude ionosphere, *Proc. IEEE*, 57, 1005-1012, 1969.
- Klumpar, D. M., *Coordinated ionospheric and magnetospheric observations from the ISIS 2 satellite by the ISIS 2 experimenters: Volume 3: High-latitude charged particle, magnetic field, and ionospheric plasma observations during northern summer*, Report No. 80-05, National Space Science Data Center, Greenbelt, Maryland, November, 1980.
- Muldrew, D. B., F-layer ionization troughs deduced from Alouette data, *J. Geophys. Res.*, 70, 2635-2650, 1965.
- Murphree, J. S., *Coordinated ionospheric and magnetospheric observations from the ISIS 2 satellite by the ISIS 2 experimenters: Volume 1: Optical auroral images and related direct*

*measurements*, Report No. 80-03, National Space Science Data Center, Greenbelt, Maryland, July, 1980.

Prikryl, P., H. G. James, D. J. Knudsen, S. C. Franchuk, H. C. Stenbaek-Nielsen, and D. D. Wallis, OEDIPUS-C topside sounding of a structured auroral E region, *J. Geophys. Res.*, in press, 1999.

Shepherd, G. G., *Coordinated ionospheric and magnetospheric observations from the ISIS 2 satellite by the ISIS 2 experimenters: Volume 2: Auroral optical emissions, magnetic field perturbations, and plasma characteristics, measured simultaneously on the same magnetic field line*, Report No. 80-09, National Space Science Data Center, Greenbelt, Maryland, December, 1980.

Sojka, J. J., W. J. Raitt, and R. W. Schunk, A theoretical study of the high-latitude winter F-region at solar minimum for low magnetic activity, *J. Geophys. Res.*, *86*, 609-621, 1981a.

Sojka, J. J., W. J. Raitt, and R. W. Schunk, Theoretical predictions for ion composition in the high-latitude winter F-region for solar minimum and low magnetic activity, *J. Geophys. Res.*, *86*, 2206-2216, 1981b.

Sojka, J. J., R. W. Schunk, W. R. Hoegy, and J. M. Grebowsky, Model and observation comparison of the universal time and IMF By dependence of the ionospheric polar hole, *Adv. Space Res.*, *11*, (10)39-(10)42, 1991.

## FIGURE CAPTIONS

Figure 1. Average location of high-latitude ionization hole [Brinton, *et al.*, 1978] and  $N_e$  cavities [Doe, *et al.*, 1993] in relation to the main trough, a representative plasma-drift configuration and a quiet-time auroral oval (adapted from Brinton *et al.* [1978] and Doe *et al.* [1993]).

Figure 2. Time intervals of ISIS-II, AE-C and DE-2 operation relative to the F10.7 solar activity. The data time intervals indicated by the numbers 1-5 correspond to the investigations of Brinton *et al.* [1978], the present ISIS-II study, Doe *et al.* [1993], Crowley *et al.* [1993], and Hoegy and Grebowsky [1991], respectively.

Figure 3. Resolute-Bay ISIS-II ionograms recorded poleward of (top: 1858:39 UT), within (middle: 1902:11 UT), and equatorward of (bottom: 1904:19 UT) a polar hole encounter on day 354 of 1976. Each ionogram is a mix of fixed (0.48 MHz) and swept (0.1 to 10.0 MHz) frequency operation.

Figure 4. Electron-density profiles deduced from the ionograms in Figure 3 corresponding to ISIS-II locations poleward of (solid curve corresponding to 1858:39 UT), within (dotted curve corresponding to 1902:11 UT), and equatorward of (dashed curve corresponding to 1904:19 UT) the polar hole (1976, day 354).

Figure 5.  $N_e$  contours (top - with ISIS-II altitude indicated by open circles),  $N_e$  (max) (middle) and  $h_{\max}$  (bottom) corresponding to days 354 (left column), 355 (center column) and 357 (right column) of 1976. The contours in the top panels correspond to  $N_e$  (max) =  $10^5$ ,  $3 \times 10^4$ ,  $10^4$  cm<sup>-3</sup>,

etc. The horizontal dashed lines in the middle panels correspond to  $5 \times 10^4 \text{ cm}^{-3}$  and provide a reference level for comparisons between passes. The horizontal dashed lines at 310 km in the bottom panels correspond to the AE-C altitude at the time of the *Brinton et al.* [1978] study.

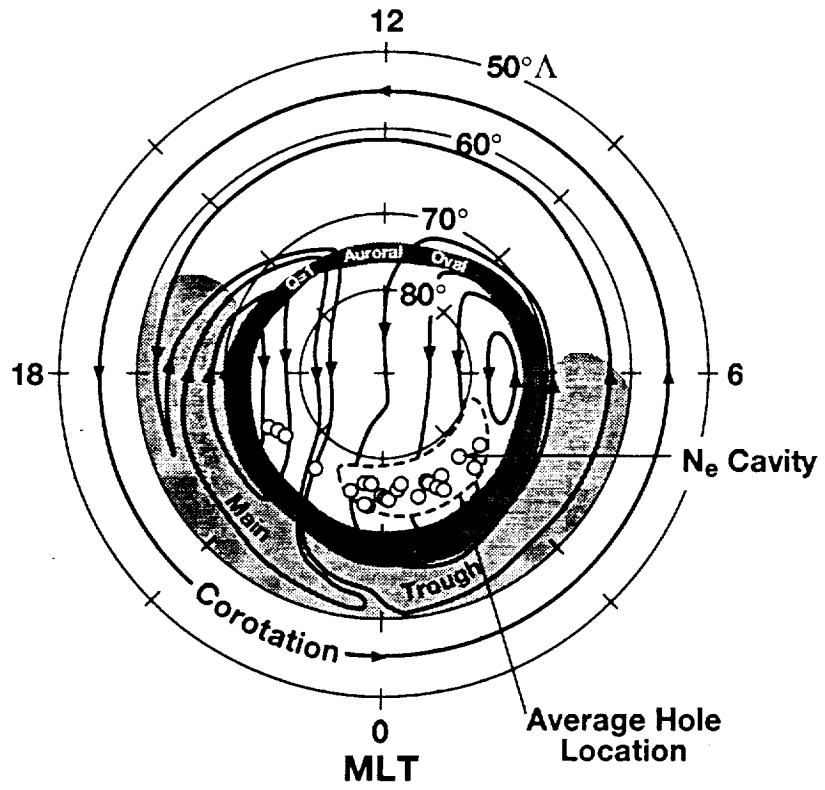


Figure 1



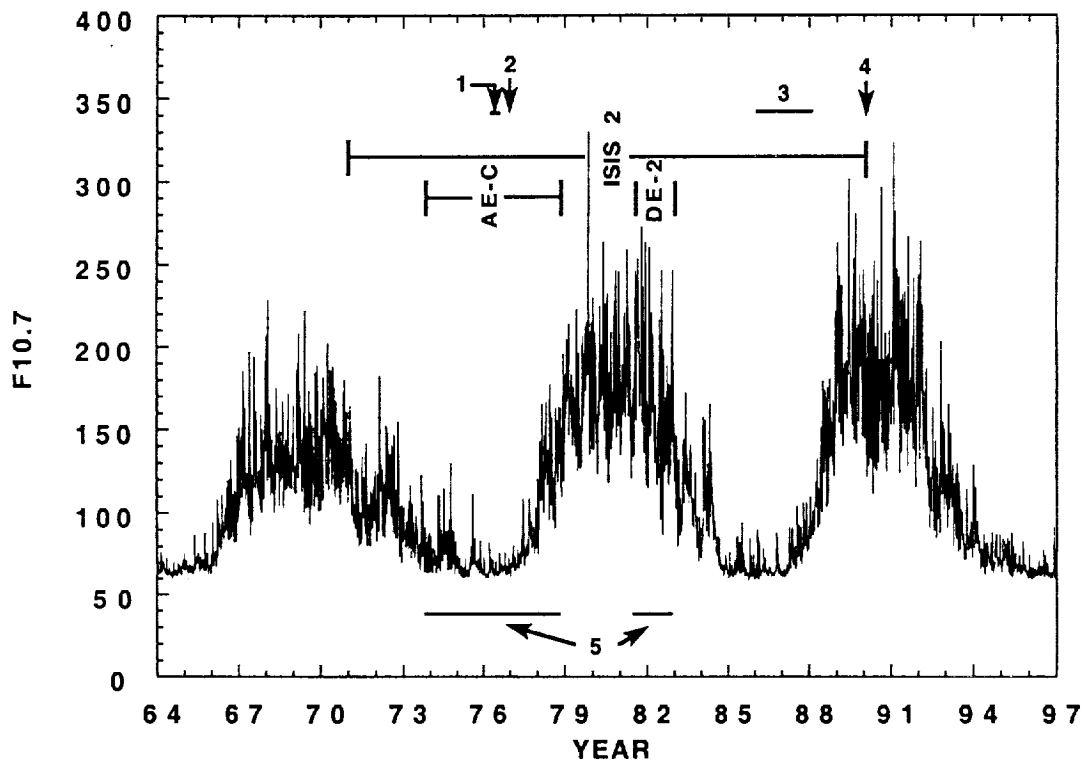


Figure 2

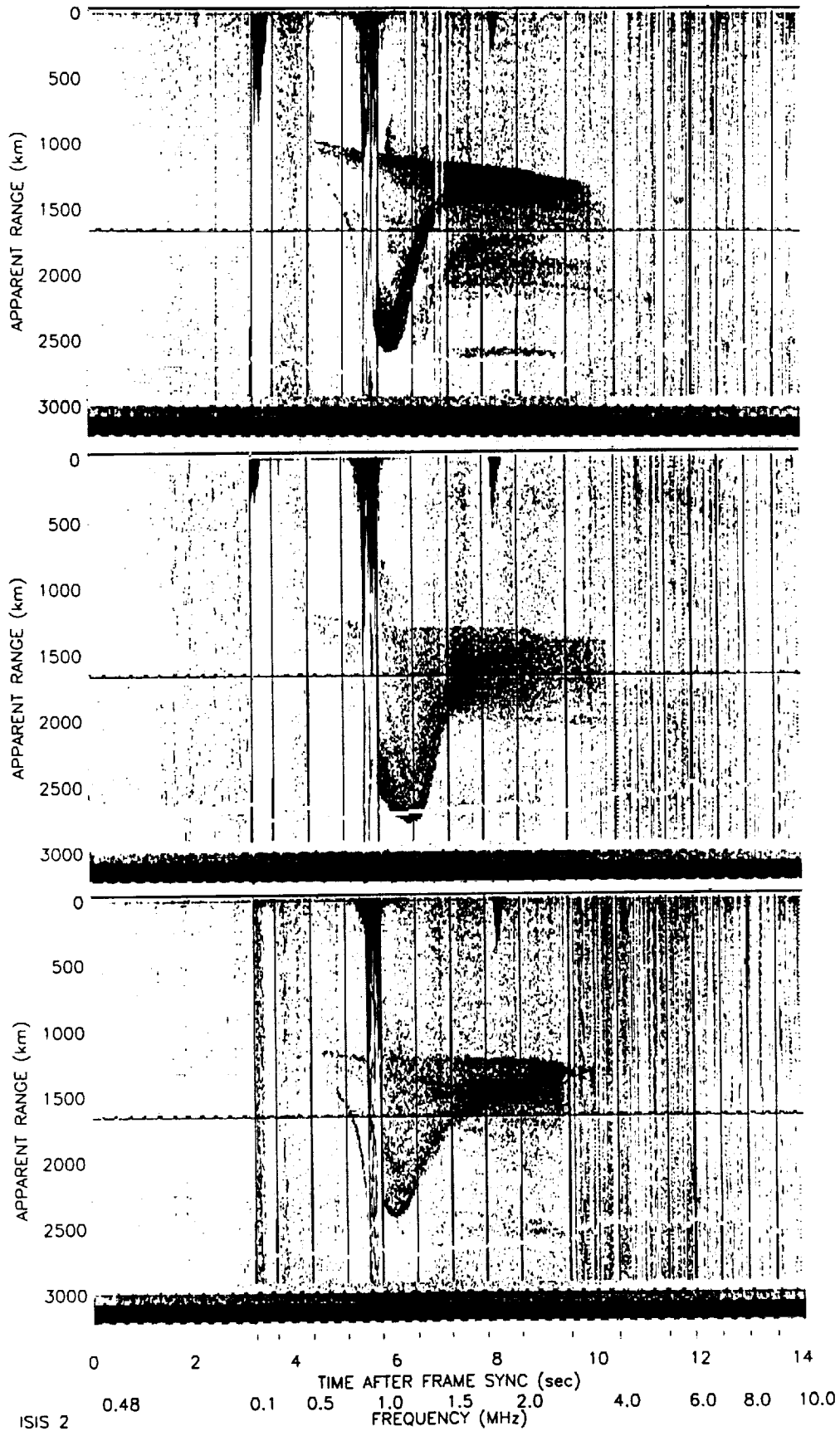


Figure 3

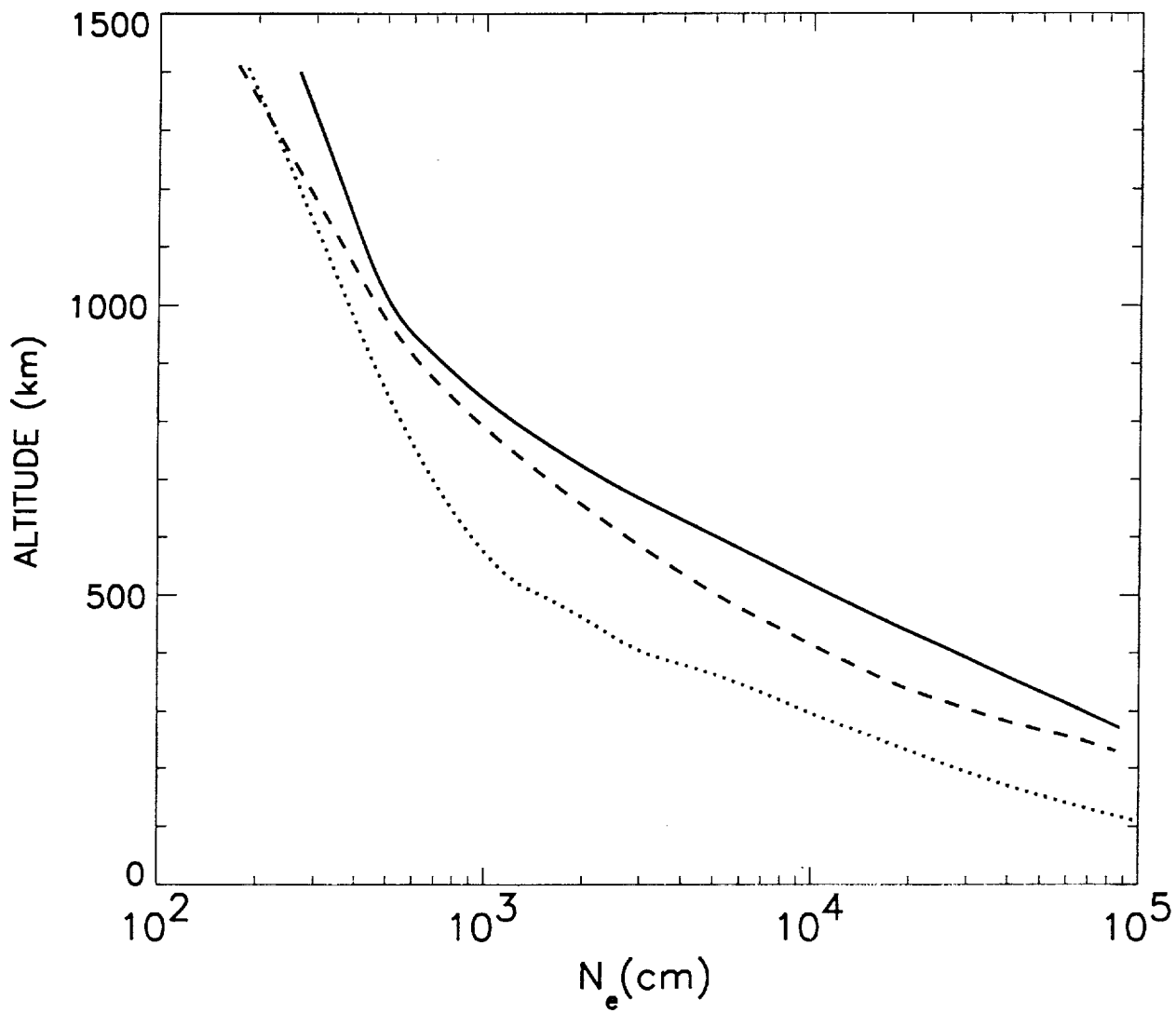


Figure 4

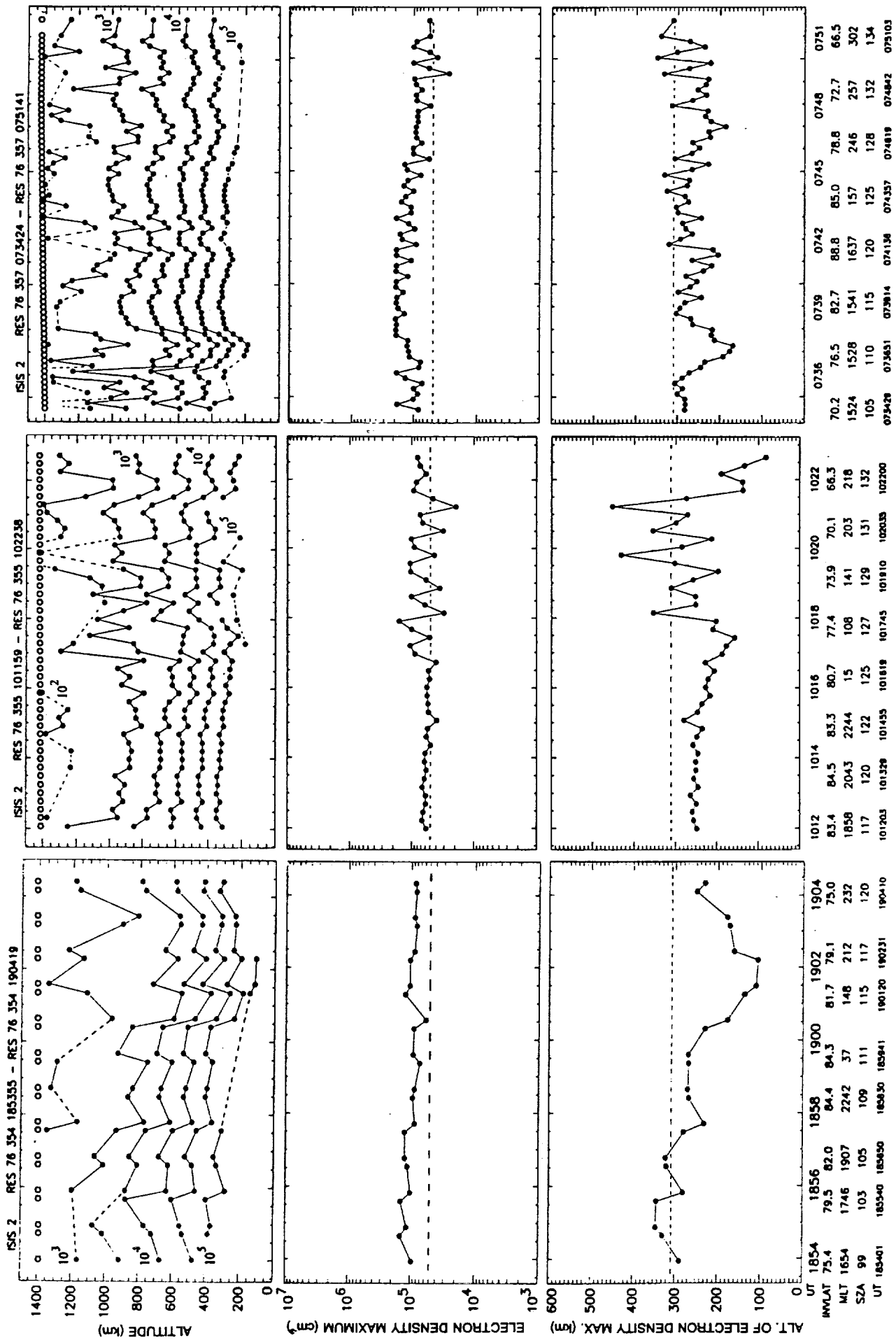


Figure 5